CO_2 Adsorption

DOI: 10.1002/anie.201207808

Mechanism of Carbon Dioxide Adsorption in a Highly Selective Coordination Network Supported by Direct Structural Evidence**

Anna M. Plonka, Debasis Banerjee, William R. Woerner, Zhijuan Zhang, Nour Nijem, Yves J. Chabal, Jing Li, and John B. Parise**

Understanding the interactions between adsorbed gas molecules and a pore surface at molecular level is vital to exploration and attempts at rational development of gas-selective nanoporous solids. Much current work focuses on the design of functionalized metal–organic frameworks (MOFs) or coordination networks (CNs) that selectively adsorb CO_2.[1–9] While interactions between CO_2 molecules and the π clouds of aromatic linkers in MOFs under ambient conditions have been explored theoretically, no direct structure evidence of such interactions are reported to date. Here we provide the first structural insight of such interactions in a porous calcium based CN using single-crystal X-ray diffraction methods, supported by powder diffraction coupled with differential scanning calorimetry (DSC-XRD), in situ IR/Raman spectroscopy, and molecular simulation data. We further postulate that such interactions are responsible for the high CO_2/N_2 adsorption selectivity, even in the case of a high relative humidity (RH). Our data suggest that the key interaction responsible for such selectivity, the room-temperature stability and the relative insensitivity to the RH of the CO_2-CN adduct, is between two phenyl rings of the linker in the CN and the molecular quadrupole of CO_2. The specific geometry of the linker molecule results in a "pocket" where carbon from the CO_2 molecule is placed between two centroids of the aromatic ring. Our experimental confirmation of this variation on theoretically postulated interactions between CO_2 and a phenyl ring will promote the search for other CNs containing phenyl ring pockets.

Selective adsorption and sequestration of CO_2 from sources of anthropogenic emissions, such as untreated waste from flue gas and products of the water gas shift reaction, is important to mitigate the growing level of atmospheric CO_2.[10] Current separation methods use absorption in alkanolamine solutions, which are toxic, corrosive, and require significant energy for their regeneration.[10] Hence microporous solid-state adsorbents, such as zeolites,[11] hybrid zeolite–polymer systems,[12] porous organic materials,[13] and MOFs[6] are proposed as alternatives, especially in combination with pressure swing processes.[14] Rather than relying solely on tuning the pore diameters of microporous materials to select between gases based on size (the kinetic diameters of CO_2, CH_4 and N_2 are 3.30, 3.76 3.64 Å, respectively[6]) selective separation relies on differences in electronic properties, such as the quadrupole moment and polarizability. Attempts to produce MOFs or CNs with adsorption properties competitive with those of commercially established aluminosilicate zeolites, relies on strategies that include pore surface modification with strongly polarizing functional groups, such as amines[2,3,5,7,9,15] and desolvating metals centers[1,3,6,8,16] to produce low-coordinated sites suitable for CO_2 adsorption. The amine-functionalized materials offer a high selectivity toward CO_2 adsorption, but a low effective surface area and thus, a low total uptake capacity.[6,17] Strong interactions with polarizing functional groups, as well as with open metal sites presents other drawbacks including an increase in the costs for material regeneration.[6] Furthermore, water effectively competes with CO_2 at low-coordinated cation sites, impeding the performance of frameworks in commercial flue gas.[6,18,19]

We recently described a porous framework, CaSDB (SDB: sulfonyldibenzoate, compound **1**) with a high CO_2/N_2 selectivity.[20] At 0.15 bar of CO_2 and 0.85 bar of N_2, a typical composition of flue gas mixture from power plants, the selectivity is in the range of 48 to 85 at 298 K. CaSDB shows a reversible uptake of CO_2 of 5.75 wt% at 273 K and 1 bar pressure and 4.37 wt% at room temperature, with heats of adsorption for CO_2 and N_2 of 31 and 19 kJ mol^{-1}, respectively. The as-synthesized compound contains not coordinated water molecules and is easily activated for gas adsorption by heating to 563 K in vacuum; remarkably the activated framework does not readsorb water, even if exposed to a RH greater than

[*] A. M. Plonka, W. R. Woerner, Prof. Dr. J. B. Parise
Department of Geosciences, Stony Brook University
Stony Brook, NY 11794-2100 (USA)
E-mail: john.parise@stonybrook.edu
Dr. D. Banerjee
Department of Chemistry, Stony Brook University
Stony Brook, NY 11794-3400 (USA)
Z. Zhang, Prof. Dr. J. Li
Department of Chemistry and Chemical Biology, Rutgers University
Piscataway, NJ 08854 (USA)
E-mail: jingli@rutgers.edu
N. Nijem, Prof. Dr. Y. J. Chabal
Department of Material Science and Engineering
University of Texas-Dallas, Richardson, TX 75080 (USA)

[**] The synthesis, structural analysis, single-crystal X-ray diffraction supported by powder diffraction coupled with differential scanning calorimetry, and preparation of the manuscript at Stony Brook is supported by the U.S. Department of Energy, Office of Science, Office of Basic Energy Sciences, under contract number DE-FG02-09ER46650. Crystal structures were determined using the Stony Brook University single-crystal diffractometer, obtained through the support of the NSF (grant number CHE-0840483). The theoretical calculations and spectroscopic measurements performed by the RU and UTD teams were supported by the U.S. Department of Energy, Office of Science, Office of Basic Energy Sciences through grant number DE-FG02-08ER46491.

Supporting information for this article is available on the WWW under http://dx.doi.org/10.1002/anie.201207808.

85%. The structure contains neither open metal sites, nor additional functionalities generally associated with sites for selective CO_2 sorption in the current literature[6] (Figure S1), raising questions of the structural origin for the selectivity of CaSDB.

In this work we employ single-crystal X-ray diffraction techniques to solve the crystal structure of a **1**:CO_2 adduct at 110 K and room temperature. In combination with powder X-ray diffraction (XRD), Raman and IR spectroscopy, theoretical calculations and real-time DSC-XRD, the CO_2 adsorbate molecules in compound **1** are accurately located. We find that the unique architecture of the SDB linkers is responsible for the strong affinity to CO_2. Prior to the collection of single-crystal XRD data, activated crystals of **1** were exposed to CO_2 in a closed container, followed by retrieval after coating in paratone oil. CO_2 is retained within the channels for at least a week and this allowed the location of gas adsorption sites within the framework from calculations of Fourier difference maps (Figure 1a). Room-temperature data were collected

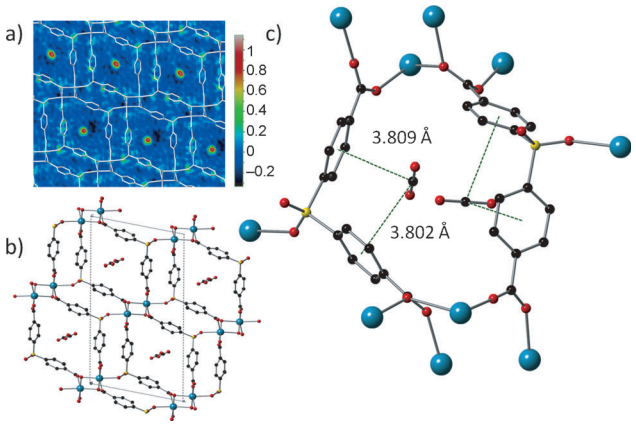

Figure 1. X-ray structure of CO_2 bound in CaSDB. a) The difference electron density map calculated before assigning CO_2 showing the carbon dioxide inside the channel (oxygen atoms are above and below the plane), the white wire represents the superimposed structure of the CaSDB framework. b) Packing along [010] showing the location of CO_2; blue spheres: calcium, red: oxygen, black: carbon, and yellow: sulfur. Hydrogen atoms are omitted for clarity. c) Local environment of the adsorbed CO_2. Dashed lines represent phenyl••••CO_2 π quadrupole interactions. The CO_2 molecule occupies two equivalent positions, with 32% occupancy on each.

just after retrieval of the crystal, while the low T data were collected from a different crystal after a week of storage in an oil. Surprisingly, the localization of the CO_2 molecules is in agreement in both cases, suggestive of a strong interaction between CO_2 and the framework. Because of its higher quality, the structure model derived from the dataset collected at 110 K will be used for discussions of the structural features responsible for the CO_2 selectivity.

The mainly observed interaction between the CO_2 molecule and the pore surface of compound **1** appears to be between the delocalized π aromatic system of both phenyl rings of the linker and the molecular quadrupole of CO_2 (Figure 1c). The specific geometry of the sulfonyldibenzoate results in a "pocket" where carbon from the CO_2 molecule is placed between two centroids of the aromatic rings at an average distance of 3.81 Å (Figure 1c). The molecule is oriented approximately parallel to both phenyl rings, keeping oxygen atoms as far as possible from their centroids, at averaged distances of 3.66 (O1C) and 4.26 Å (O2C). This configuration keeps both oxygen atoms relatively close to two hydrogen atoms, at average distances of 3.89 and 3.85 Å for O1C and O2C, respectively. The CO_2 molecules adopt two positions approximately in the middle of the channel, binding to one of the linkers, which are averaged in diffraction data, thus maintaining the $P2_1/n$ space group of the structure (Figure 1b). The occupancy of the CO_2 molecule was refined to be 32% and no spatial disorder is shown.

The distance and parallel configuration of the aromatic ring and the CO_2 molecule observed in **1** is in good agreement with reported theoretical studies on single phenyl rings.[15] However, the calculated heat of adsorption for CO_2 in CaSDB (<-30 kJ mol^{-1} [20]) is significantly lower than the predicted -5.6 kJ mol^{-1} for the molecular benzene–CO_2 complex. This higher interaction energy is most probably the result of simultaneous interactions with two rings, coupled with the influence of additional hydrogen atoms and possibly an overall effect of the small pores, which allows for a weak interaction with the other linker. The structure of the **1**:CO_2 adduct suggests that the selective sorption of CO_2 over N_2 is displayed by compound **1** beause of the large quadrupole moment of CO_2 (43.0×10^{-27} esu^{-1} cm^{-1}) compared to that of N_2 (15.2×10^{-27} esu^{-1} cm^{-1}).

Our observation that the activated form of **1** does not readsorb water from the atmosphere and adsorbs CO_2 strongly enough to allow for structure determination, suggested that **1** may retain a selectivity at high RH. Simultaneous DSC-XRD is a very effective means of correlating thermal signatures with structural response. We observed the DSC-XRD signatures for CO_2 adsorption at 2 and 75% RH during a gas swing adsorption experiment. During the experiment the atmosphere was alternated between flowing N_2 and CO_2 in several cycles allowing the system to equilibrate after each change. The DSC signal was recorded simultaneously with powder XRD scans, and the results show that the crystallinity and the performance of CO_2 adsorption is not diminished over at least five cycles (12 h) under either dry (2% RH) or humid conditions (75% RH; Figure 2). Measurements under both dry and humid conditions show very strong exothermic effects after changing the atmosphere from N_2 to CO_2, proving that CO_2 competes very effectively with water for adsorption at the phenyl pockets. Powder diffraction patterns recorded after equilibration in CO_2 atmosphere reveal that there is no major structural change in CaSDB when CO_2 is introduced, but that the low angle peaks $10\bar{1}$, 002, and 101 reproducibly decrease in comparison to the rest of the pattern suggesting that CO_2 occupies space within the pore, consistent with the proposed CO_2 adsorption mechanism (Figure S3).

Vacuum swing DSC measurements were used to determine the differential enthalpy between the empty pore and the gas-loaded (N_2 and CO_2) CaSDB under ambient conditions. The measured differential enthalpy of adsorption was 10.221(81) and 0.779(26) kJ mol^{-1} for CO_2 and N_2, respec-

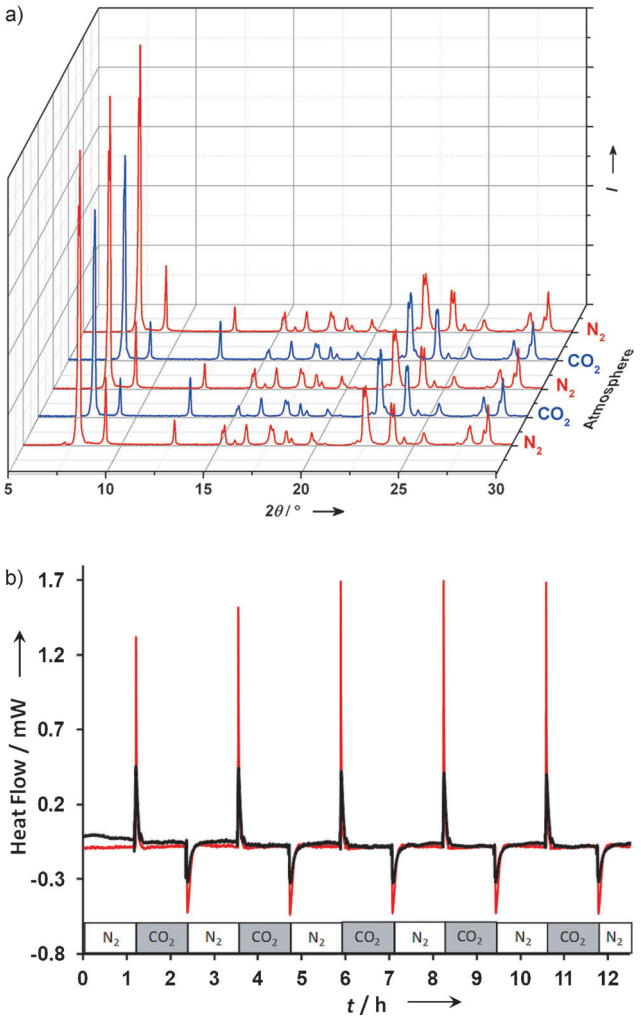

Figure 2. Gas swing experiment for CO_2 loading in the CaSDB framework. a) XRD patterns (background subtracted) at 2% RH showing the change in relative intensities of low-angle peaks under the different conditions. b) Strong exothermic and endothermic effects for experiments performed in 2% RH (red) and 75% RH (black) at 298 K.

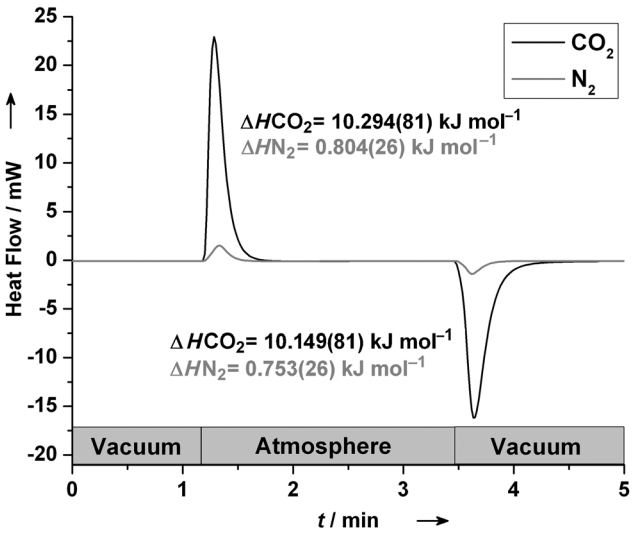

Figure 3. Vacuum swing adsorption DSC data for one cycle of CO_2 and N_2 loading/unloading in the CaSDB framework.

tively (Figure 3). At 1 atm pressure and room temperature, the weight percentage of CO_2 and N_2 adsorbed is 4.5 and 0.3, with isosteric heat of adsorption (Q_{st}) values of 30 and 22 kJ mol^{-1}, respectively.[20] This yields a calculated enthalpy of adsorption (H) of 0.811 kJ mol^{-1} for N_2 and 10.56 kJ mol^{-1} for CO_2 when using the relation of $H = Q_{st} n_i$ (n_i = moles of the gas). The measured and calculated values are in very good agreement, which confirms that the vacuum swing DSC measurements provide valid results useful for judging the activity of the compound for gas adsorption. This method can be applied as a screening technique to other compounds and gases as well.

Apart from crystallographic methods we sought further insight into the adsorption mechanism by carrying out grand canonical Monte Carlo simulations and spectroscopic observations; the results are in good agreement with the described mechanism (see the Supporting Information).

Determining the key interactions responsible for selectivity is vital to the development of reliable interatomic potentials necessary for simulating the adsorption behavior and for providing insights to stimulate further exploratory synthesis. For zeolite molecular sieves this approach allows routine prediction of adsorption behavior.[21] Repeating this success for crystalline MOFs/CNs requires high-quality XRD data to precisely identify adsorption sites, and to augment the still limited number of structural reports on CO_2 adsorbed in nanoporous hybrid materials. Most reports focus on the interaction between CO_2 and low-coordinated cations or additional functionalities inside the framework.[1,2,4,5,7,9] In this context our study describing CO_2–phenyl ring interactions in an alkaline-metal-containing CN is novel and encouraging in the search for alternative mechanisms for CO_2 selectivity.

Experimental Section

Single-crystal XRD with adsorbed CO_2: Compound $\mathbf{1}{\cdot}H_2O$ was synthesized by solvothermal methods and activated by vacuum heating as described previously.[23] During vacuum heating the compound transformed to the activated phase.[20] Analysis of single-crystal diffraction data did not reveal any significant residual electron density remaining inside the channels. The activated compound was then placed together with pieces of solid CO_2 into a 37 mL teflon bottle sealed with parafilm. After an hour the material was taken out and coated with paratone. The crystals were analyzed under an optical microscope, fitted with polarizing optics, and high-quality single-crystals were chosen for structural analysis.

Reflections for the CO_2 loaded compound were collected using a four-circle kappa Oxford Gemini diffractometer equipped with an Atlas detector ($\lambda = 0.71073$ Å) with 1° ω scans at 110 K. The raw intensity data were collected, integrated, and corrected for absorption effects using CrysAlis PRO software.[22]

The crystal structure of compound $\mathbf{1}{\cdot}(CO_2)_{0.32}$ was solved using direct methods (SHELXS).[23] All of the non-hydrogen atoms were refined anisotropically (Figure S2). Hydrogen atoms were added to the structure model using geometrical constraints. The position for the CO_2 molecule was located in Fourier difference maps. The occupancy of the atoms in CO_2 was refined to 32%. The CO bond

length was constrained to 1.16 Å. A summary of some important crystallographic details can be found in Table S1. CCDC 900050 contains the supplementary crystallographic data for this paper. These data can be obtained free of charge from The Cambridge Crystallographic Data Centre via www.ccdc.cam.ac.uk/data_request/cif.

XRD-DSC measurements: The powder XRD measurements were conducted using a Rigaku Ultimia IV diffractometer with a D/teX ultrahigh speed position sensitive detector. Two different stages were used during the data collection, an XRD-DSC stage and a low/medium temperature stage. The XRD-DSC stage allows for simultaneous collection of XRD and DSC data in a controlled atmosphere. A humidity generator (Rigaku HUM-1) was used to control the humidity of the atmosphere at each stage during the collection of data. The DSC measurements were performed using 9.6 mg of the sample in an aluminum crucible with an equal amount of Al_2O_3 in the reference crucible. The reported XRD patterns (Figure 2, top) were later collected using the low/medium temperature Rigaku stage and the results agreed with the first measurement with the DSC stage. The low/medium temperature stage allows for a controlled atmosphere as for the XRD-DSC stage but provides XRD patterns of a higher quality.

For the vacuum and gas swing experiments the sample was first heated to 573 K under vacuum on the XRD-DSC stage and held at 573 K for 8 h to ensure the activation and then cooled to room temperature. For the vacuum swing experiment the chamber was then pressurized to 1 atm of CO_2 over the course of 10 seconds. After 2 minutes, when the DSC signal returned to the baseline, the chamber was then evacuated to rough vacuum over the course of ten seconds. A total of ten cycles was completed. In the gas swing experiment the activated sample was exposed to an N_2 atmosphere at a constant flow rate of 50 mL min^{-1} until the DSC signal returned to the baseline and then the atmosphere was switched to CO_2 and kept for an hour. The changes were made every hour for 12 h.

Received: September 27, 2012
Published online: December 11, 2012

Keywords: CO_2 adsorption · metal–organic frameworks · X-ray diffraction

[1] P. D. C. Dietzel, R. E. Johnsen, H. Fjellvag, S. Bordiga, E. Groppo, S. Chavan, R. Blom, *Chem. Commun.* **2008**, 5125 – 5127.
[2] J. B. Lin, W. Xue, J. P. Zhang, X. M. Chen, *Chem. Commun.* **2011**, *47*, 926 – 928.
[3] B. Li, et al., *Angew. Chem.* **2012**, *124*, 1441 – 1444; *Angew. Chem. Int. Ed.* **2012**, *51*, 1412 – 1415.
[4] C. Serre, et al., *Adv. Mater.* **2007**, *19*, 2246 – 2251.
[5] E. Stavitski, E. A. Pidko, S. Couck, T. Remy, E. J. M. Hensen, B. M. Weckhuysen, J. Denayer, J. Gascon, F. Kapteijn, *Langmuir* **2011**, *27*, 3970 – 3976.
[6] K. Sumida, D. L. Rogow, J. A. Mason, T. M. McDonald, E. D. Bloch, Z. R. Herm, T.-H. Bae, J. R. Long, *Chem. Rev.* **2012**, *112*, 724 – 781.
[7] R. Vaidhyanathan, S. S. Iremonger, G. K. H. Shimizu, P. G. Boyd, S. Alavi, T. K. Woo, *Science* **2010**, *330*, 650 – 653.
[8] H. Wu, J. M. Simmons, G. Srinivas, W. Zhou, T. Yildirim, *J. Phys. Chem. Lett.* **2010**, *1*, 1946 – 1951.
[9] J. P. Zhang, X. M. Chen, *J. Am. Chem. Soc.* **2009**, *131*, 5516 – 5521.
[10] B. Metz, D. Ogulande, H. de Connick, M. Loos, L. Meyer, Cambridge University Press, New York, **2005**.
[11] J. C. White, P. K. Dutta, K. Shqau, K. H. Verweij, *Langmuir* **2010**, *26*, 10287 – 10293.
[12] M. D. Determan, D. C. Hoysall, S. Garimella, *Ind. Eng. Chem. Res.* **2012**, *51*, 495 – 502.
[13] J. Tian, P. Thallapally, J. Liu, G. J. Exarhos, J. L. Atwood, *Chem. Commun.* **2011**, *47*, 701 – 703.
[14] T. L. P. Dantas, F. M. T. Luna, I. J. Silva Jr., A. E. B. Torres, D. C. S. de Azevedo, A. E. Rodrigues, R. F. P. M. Moreira, *Chem. Eng.* **2011**, *172*, 698 – 704.
[15] A. Torrisi, C. Mellot-Draznieks, R. G. Bell, *J. Chem. Phys.* **2009**, *130*, 194703.
[16] D. Banerjee, J. B. Parise, *Cryst. Growth Des.* **2011**, *11*, 4704 – 4720.
[17] R. Krishna, J. M. van Baten, *Sep. Purif. Technol.* **2012**, *87*, 120 – 126.
[18] A. C. Kizzie, A. G. Wong-Foy, A. J. Matzger, *Langmuir* **2011**, *27*, 6368 – 6373.
[19] J. Liu, Y. Wang, A. I. Benin, P. Jakubczak, R. R. Willis, M. D. LeVan, *Langmuir* **2010**, *26*, 14301 – 14307.
[20] D. Banerjee, Z. Zhang, A. M. Plonka, J. Li, J. B. Parise, *Cryst. Growth Des.* **2012**, *12*, 2162 – 2165.
[21] P. A. Wright, J. M. Thomas, A. K. Cheetham, A. K. Nowak, *Nature* **1985**, *318*, 611 – 614.
[22] CrysAlis PRO. Verion 4. Oxford Diffraction Ltd. Yarnton, Oxfordshire, England, **2010**.
[23] G. M. Sheldrick, *Acta Crystallogr. Sect. A* **2008**, *64*, 112 – 122.

